Chapter 21
Fabrication and Analysis of Apparatus for Measuring Stored Renewable Hydrogen Energy in Metal Hydrides

Rohan Kalamkar, Vivek Yakkundi, and Aneesh Gangal

Introduction

Hydrogen is considered as futuristic fuel for next-generation vehicles based on Polymer Electrolyte Membrane Fuel Cell (PEMFC) [1]. PEMFC translates the chemical energy of hydrogen directly into electrical energy [2, 3]. Hydrogen has a high average heating value, i.e., 120 MJ/kg of H_2 [4]. It is necessary to have a hydrogen storage mode and mechanism to deliver this energy in a usable form. For sourcing electrical power to the applications, a fuel cell is used as a battery [5]. The average gravimetric energy density of hydrogen is 120 MJ/Kg, compared with the energy density of petrol, which is 44 MJ/Kg. The volumetric density of hydrogen is sparse with 0.01 MJ/L [6] compared with 32 MJ/L of petrol. The energy required to ignite a hydrogen–air mixture is very low only 0.02 MJ, which is about one-fourteenth of the energy needed to ignite natural gas [7]. For establishing realistic hydrogen storage technologies, a 9 wt% gravimetric storage objective has been proposed for hydrogen-powered vehicles by the US Department of Energy for attaining a 500 km driving range [8]. However, the materials tested so far did not even reach close to the DOE set targets. Figure 21.1 shows a block diagram of the working of PEMFC.

R. Kalamkar (✉)
Mechanical Engineering Department, Gharda Institute of Technology, Lavel, India
e-mail: rohanhirve@gmail.com

V. Yakkundi
Mechanical Engineering Department, Lokmanya Tilak College of Engineering, Navi Mumbai, India
e-mail: vivek.yakkundi@gmail.com

A. Gangal
Mechanical Engineering Department, SSPM's College of Engineering, Kankavali, India
e-mail: aneeshgangal@gmail.com

S. Kumar and K. P. Rajurkar (eds.), *Advances in Manufacturing Systems*,
Lecture Notes in Mechanical Engineering,
https://doi.org/10.1007/978-981-33-4466-2_21

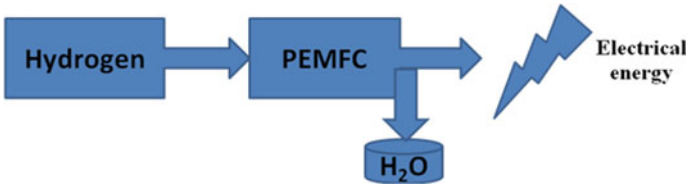

Fig. 21.1 Block diagram of working of PEMFC

The storage of hydrogen is possible as compressed gas, liquid at cryogenic temperature, or solid-state hydride phase. Pressure vessels commercially available are either of 5000 and 10,000 psi compressed hydrogen [9]. The energy density of hydrogen can be doubled as compared to the 10,000 psi compressed hydrogen to 70 g/L by liquefaction to the temperature of 20 K [10]. Thus the high pressure compressed hydrogen storage has issues concerning the strength of the material, the safety of the tank, and finally, the tank weight, while the issues with liquid hydrogen storage are the boil-off loss and the energy requirements for liquefaction. However, both these issues are addressed in solid-state hydrogen storage where hydrogen combines either physically or chemically with some of the materials to give hydrides and hydrogen can be obtained whenever required by either thermal stimulation or some other technique like hydrolysis [11].

This work consists of the fabrication of experimental setup to measure stored renewable hydrogen energy in solid metal hydrides. This experimental setup evaluates the absorption/desorption kinetics of sample materials based on a volumetric approach. The working range of this fabricated of the experimental setup is 0.05–50 bar pressure and 300–723 K temperature. It comprises of a reactor for the interactivity of hydrogen gas with the solid sample material and measuring cell to examine the weight% capacity of hydrogen storage [12]. The fabricated system has a volume of 150 cm^3 having 100 bar internal pressure capacity. The setup is made up of stainless steel material with a high-resolution pressure transducer. The wt% capacity of stored hydrogen is determined using van der Waals equation for a real gas. The effect of ball-milled sample materials on the magnification of hydrogen wt% reported in this work. This research study also describes the outcome of additive Zeolite on enhancement in hydrogen capacity with a reduction in reaction temperature. Characterization is done using Fourier-transform infrared spectroscopy (FTIR) and Transmission electron microscopy (TEM) spectroscopy methods for validation.

Experimental

Sievert's type apparatus fabricated to measure hydrogen stored in solid-state powder materials. The instrument uses a volumetric method to determine wt% of stored hydrogen. The device works within a range of 0.05–50 bar pressure and 300–723 K temperature. The pressure sensor takes an input of 9–30 V DC and provides an

outcome of 4–20 mA. The K type thermocouples are used with two-wire legs welded together at for temperature measurement at a junction. This experimental setup comprises a vacuum system of 10^{-5} mbar range to remove gas molecules from a system. The pressure change in the system corresponds to the hydrogen concentration of the sample material [13]. The temperature of a gas, system volume and pressure change in the system used as data for the van der Waals equation for finding out wt% H_2 stored [14, 15]. For the estimation of concealed volumes in the system, the gas expansion method was used. Figure 21.2 represents (a) conceptual apparatus schematic diagram and (b) shows the photograph of the fabricated experimental setup.

The outcome of this measurement is pressure composition (PC) isotherms graphs, which designate the characteristics of the sample material. The graph consists of α—region corresponds to the starting of hydride formation, β—region specifies an increase in the concentration of hydrogen, and the third region is the saturation phase. The constant pressure, i.e., plateau region in the graph, represents the equilibrium pressure of hydrogen [16]. Figure 21.3 illustrates an ideal PC isotherm.

The tubing and the reactor volume estimated using the calibration of the experimental setup before performing the experiments. In an indirect method of gas expansion, the standard cell of size 350 cc was used. Equation 21.1 represents van der Waals equation for a real gas.

$$\left(P + \frac{\mathrm{n}^2 a}{\mathrm{V}^2}\right)(V - nb) = n\mathrm{RT} \tag{21.1}$$

The a is the correction for intermolecular forces, which is 0.0248 J m^3/mol^2, b is the correction for finite molecular size, which is 2.66 × 10–5 m^3/mol^2 [5]. For P1 = 7.9 bar, volume = 350 cc (0.00035 m^3) and temperature T = 298 K number of

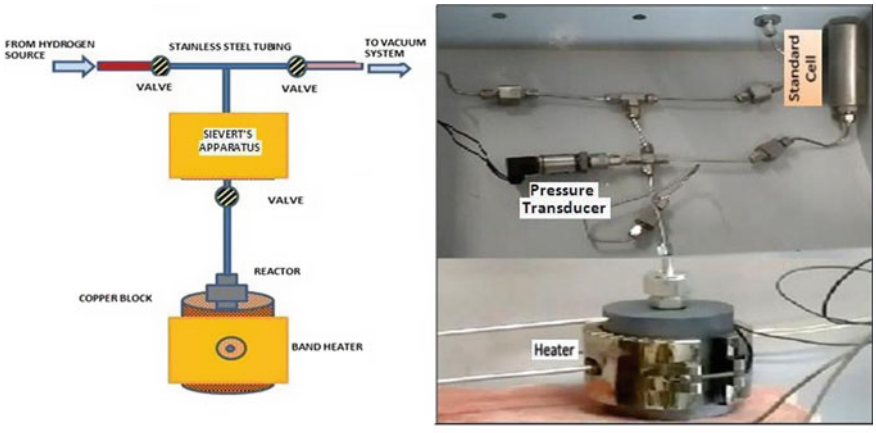

Fig. 21.2 **a** Apparatus schematic diagram. **b** Photograph of fabricated experimental setup

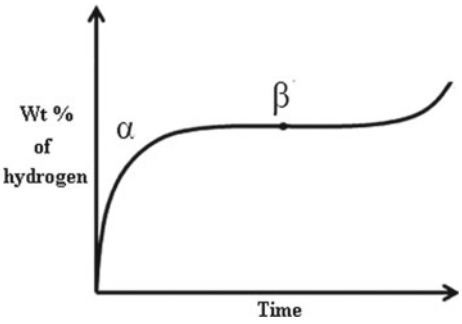

Fig. 21.3 Ideal pressure composition (PC) isotherm

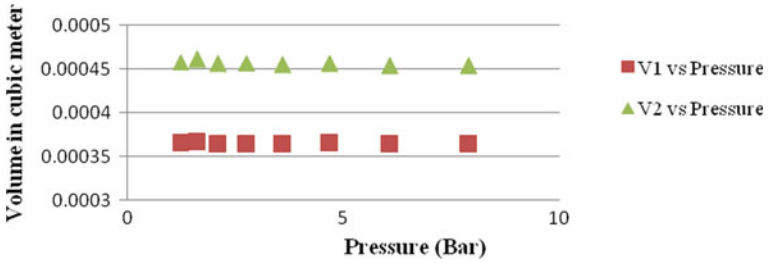

Fig. 21.4 Calibration curve

moles are calculated as N = 0.11066 from Eq. 21.1. For P2 = 7.6 bar, P3 = 6.08 bar and keeping all other parameters the same, tubing volume as 14 cc and the reactor volume as 90 cc calculated. Figure 21.4 specifies the calibration curve.

Result and Discussions

In a closed material hydrogen system, the sequences of changes are observed in hydrogen pressure at the isothermal condition. Wt% of hydrogen estimated using system pressure and sample temperature. The total number of moles evaluated using van der Waals equation for a real gas. Magnesium and Aluminum crystalline powder (Sigma-Aldrich) is ball milled for 12 h. The transmission electron microscopy (TEM) technique is used for the characterization. The electron diffraction patterns of Mg and Al nanoparticles are shown in Fig. 21.5. Particle size calculated from images was approximately 60–80 nm. The images stipulate ringed pattern and differently oriented lattice fringes.

Magnesium powder is a nontoxic grey crystalline solid used for the hydrogenation test. Magnesium hydride (MgH_2) has 9 MJ/kg of energy density [17]. With low-cost available magnesium, MgH_2 has about 7.7 wt% hydrogen storage capacity [18]. Mg crystalline powder and ball-milled Mg particles were allowed to react separately

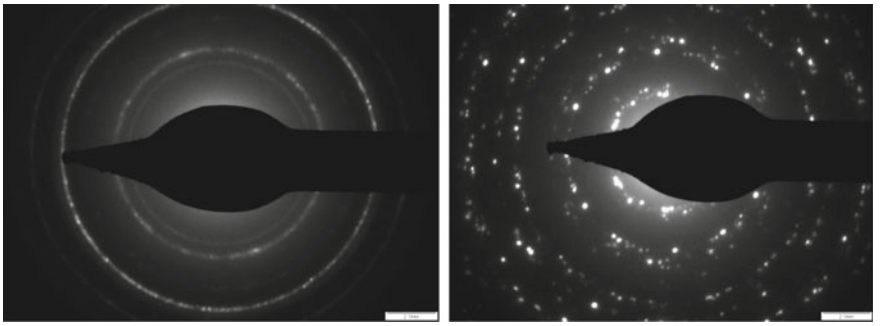

Fig. 21.5 **a** Electron diffraction pattern of Mg. **b** Electron diffraction pattern of Al

with the hydrogen gas, filled in the 350 cc cylinder at 14.5 bar pressure with constant temperature 573 K. The results plotted in the graph were average of three tests. Results show hydrogen storage of 4.38 wt% in the case of Mg crystalline powder and 5.10 wt% in the case of ball-milled Mg. Aluminum is a silvery white, soft, nonmagnetic, and ductile metal. Aluminum hydride (AlH_3) contains 10.1 wt% of hydrogen [19]. Al crystalline powder and ball-milled Al nanoparticle were allowed to react separately with the hydrogen, keeping pressure and temperature the same as in the case of Mg. Results specify hydrogen storage of 2.8 wt% in the case of Al crystalline powder and 3.7–4.0 wt% in the case of ball-milled Al nanoparticles. The outcome of the experiment stipulates that optimum time for the milling process boosts the sample's hydrogen storage capability. The peak hydrogen absorption temperature decreases slowly with decreasing the average particle size of the sample material. Figure 21.6 indicates the effect of particle size on hydrogen storage.

Zeolites are also the microporous solids widely used for adsorbents and catalysts. Zeolite is used as hydrogen storage materials, but the amount of hydrogen taken up by both these materials was not sufficient from the application point of view [20].

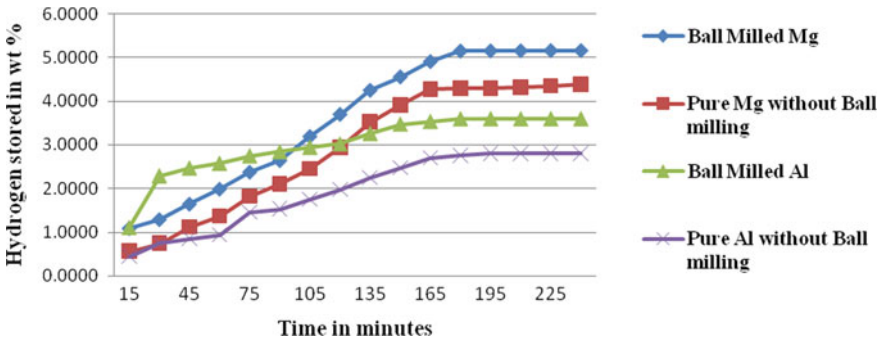

Fig. 21.6 Effect of particle size on hydrogen storage

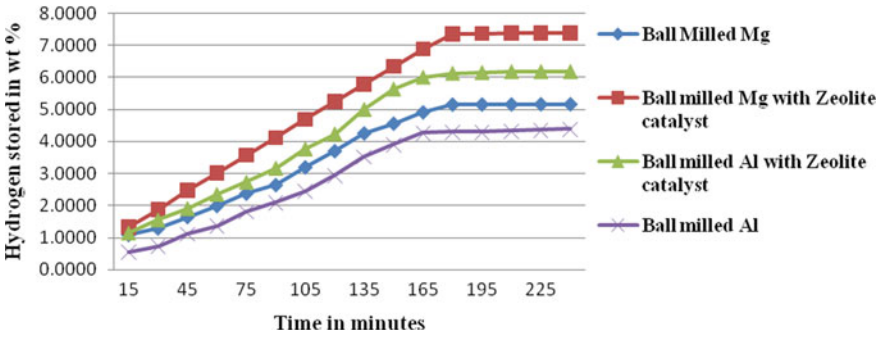

Fig. 21.7 Hydrogenation test results of Magnesium and Aluminum

This observation led to the thought that if both materials physisorbed hydrogen, it may assist hydrogenation by accelerating the reaction rate. Therefore the use of Zeolite as catalysts for hydrogenation experiments was proposed. The Zeolite (Ag_{84} Na_2 $[(AlO_2)86$ $(SiO_2)106] \times H_2O$—N.H. Chemicals) nanoparticles are mixed with Mg and Al nanoparticle in 1:10 mass ratio. Both the materials were milled for 1 h to obtain a homogenous mixture. The consequences of the addition of the catalysts were observed. The coverage and surface temperature are influencing the reactivity of Zeolite [21]. The mean test results' footprint revealed optimum hydrogen storage of 7.38 wt% at the temperature of 453 K and 14.5 bar pressure using Zeolite as a catalyst in the test. Further, the hydrogenation tests of Al nanoparticles with the hydrogen gas in the presence of Zeolite catalyst were conducted. Mean outcome indicates hydrogen storage of 6.18 wt% in Aluminum using Zeolite as a catalyst keeping all other conditions the same as in case of Mg-Zeolite hydrogenation test. Each sample test repeated thrice, and average results are represented graphically in Fig. 21.7.

Validation by Spectroscopy

Infrared radiations traveled through the samples in Fourier transform infrared spectroscopy. The characterization represents the molecular absorption/transmission, and this spectrum was unique for the molecular structure of the respective sample [22]. In this work, the FTIR transmittance spectrum [23] recorded using a Jasco FT/IR-6100A system [SAIF, IITB]. In Transmission Electron Microscopy, an electron beam focused on the samples using the condenser lens system. Magnified image and the X-ray produced through interaction were analyzed for evaluating the elemental composition [24]. Philips CM200 TEM used with voltage range 20–200 kV and the resolution of 2.8 Å [SAIF, IITB] for this work. FTIR and TEM tests conducted at IIT Bombay, SAIF laboratory facility. Figures 21.8, 21.9, 21.10 and 21.11 represent the

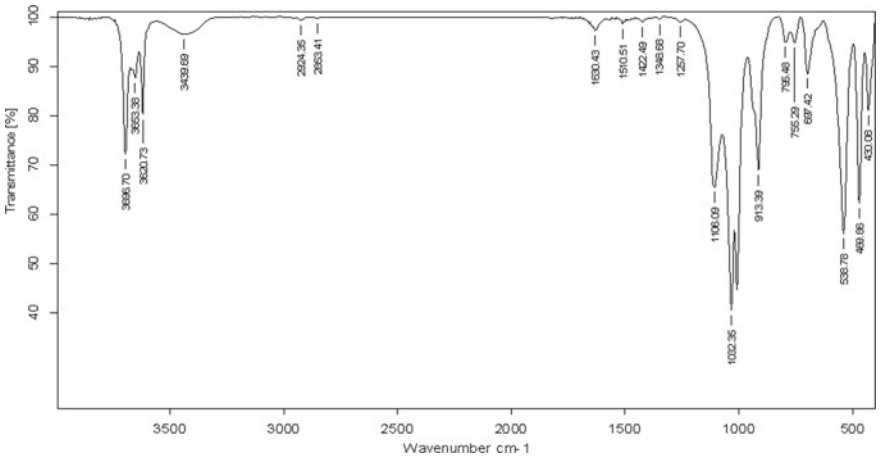

Fig. 21.8 FTIR of Mg crystalline powder

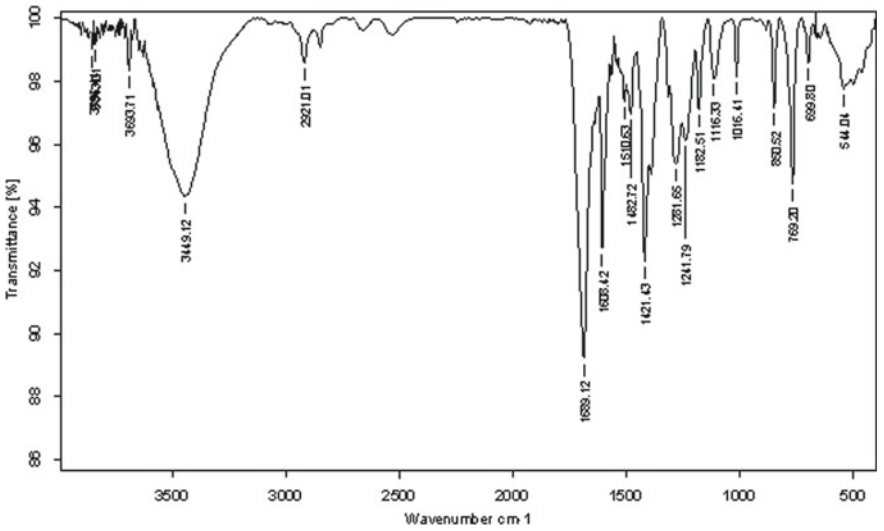

Fig. 21.9 FTIR of ball-milled Mg with Zeolite catalyst

FTIR transmittance spectra of Mg crystalline powder, ball-milled Mg with Zeolite catalyst, Al crystalline powder, ball-milled Al with Zeolite catalyst respectively.

Transmittance spectra of Mg of solid residue after hydrogenation tests with additive Zeolite depicted that the frequencies are greatly affected, i.e., stretching and wagging was observed, 1639 cm^{-1}, 1421 cm^{-1} in Mg-Zeolite and 1605 cm^{-1}, 659 cm^{-1} in Al-Zeolite solid residue. Storage of hydrogen reflects in terms of broadening of the transmittance peaks, 3449 cm^{-1}, 2921 cm^{-1} in Mg-Zeolite and

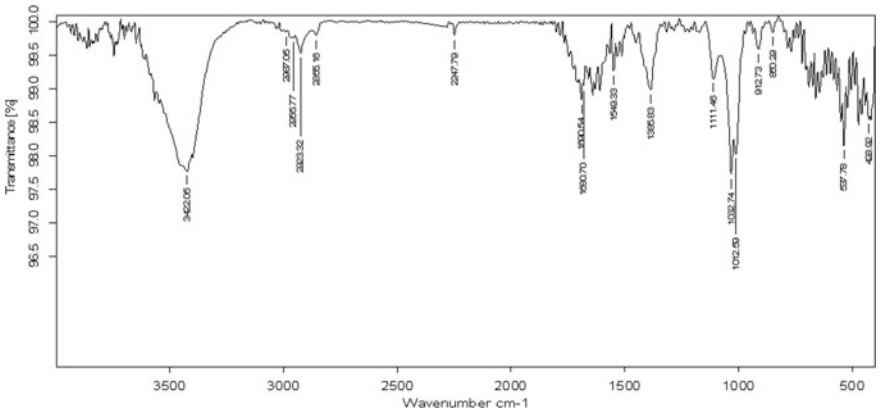

Fig. 21.10 FTIR of Al crystalline powder

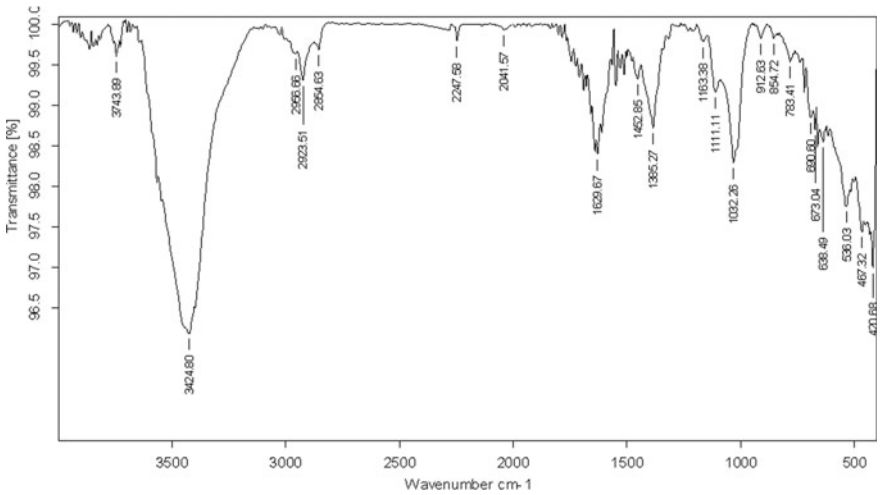

Fig. 21.11 FTIR of ball-milled Al with Zeolite catalyst

3443 cm^{-1}, 2923 cm^{-1} in Al-Zeolite solid residue when compared with the spectrum of crystalline powder. The increase in sharpness of the spectrum peak implies hydrogen absorption kinetics [25]. FTIR spectra of solid residue after tests do not show any bands corresponding to Zeolite-H which designate Zeolite additive do not take part in reactions. Figure 21.12 shows TEM images of Mg and Al sample materials. TEM images before and after hydrogenation indicate the reduction in the pores with enhancement in the intensity of dark spots/ patches. It signifies hydride formation in Mg compared with BCC-structured catalyst imbedded in the MgH_2 matrix images [26]. HRTEM images of Mg and Al with additives reflecting hydride formation [27, 28].

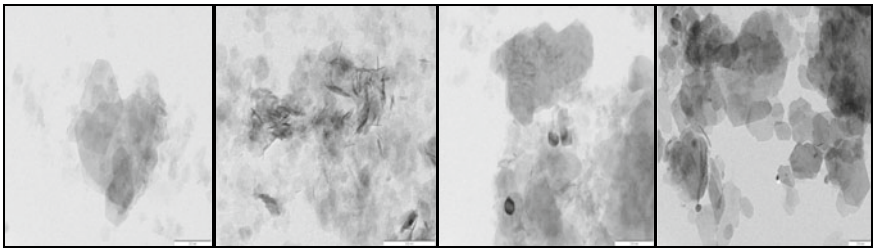

(a) (b) (c) (d)

Fig. 21.12 **a** TEM image of Mg crystalline powder. **b** TEM image of milled Mg with Zeolite. **c** TEM image of Al crystalline powder. **d** TEM image of milled Al with Zeolite

Conclusion

The analysis of the fabricated apparatus noticed experimental errors within 10% in correlation with accuracy. The lightweight metals Mg and Al suggested encouraging materials for H_2 storage, but having an issue of the slow kinetics. The hydrogenation of Mg and Al with and without Zeolite additives was made to refine the behavior. The additives enhance the net H_2 storage around 2.23 wt% in Mg and 2.10 wt% in Al using Zeolite as a catalyst during isothermal reactions. The passiveness during hydrogenation in the surface of additives increases sorption, which reflects in edges in the transmittance spectra. Additives accelerate the rate of reaction as well as decreasing the reaction temperature by 120 K in Mg and 150 K in Al. No foaming was observed with additives. Hence, the catalyst improves the reaction kinetics behavior of Magnesium. Validations of the experimental outcomes using FTIR and TEM characterization found to be similar when correlated with the previously published research articles to authenticate the experimental system.

Acknowledgements Authors are grateful to the Gharda Institute of Technology, Lavel, for the support received concerning the work presented in the paper.

References

1. Gangal AC, Kale P, Edla R (2012) Study of kinetics and thermal decomposition of ammonia borane in presence of silicon nanoparticles. Int J Hydrogen Energy 37(8):123–134
2. Kalamkar R, Yakkundi V, Gangal A (2020) Hydrogen storage characteristics of mixture of lithium amide and lithium hydride using severt's type apparatus. In: Pawar P, Ronge B, Balasubramaniam R, Vibhute A, Apte S (eds) Techno-societal 2018. Springer, Cham, pp 1037–1044
3. Gangal AC, Sharma P (2013) Kinetic analysis and modeling of thermal decomposition of Amonia borane. Int J Chem Kinet 45(7):452–461
4. Dehghani AR, Tharumalingam E (2019) Study of energy storage system and environmental challenges of batteries. Renew Sustain Energ Rev 104:192–208

5. Gangal A (2013) Ammonia borane as hydrogen storage material. Thesis. Department of Energy Science & Engineering IIT Bombay
6. Zuttel A (2004) Hydrogen storage methods. Naturwissenschaften 91(4):157–172
7. Zuttel A (2003) Materials for hydrogen storage. Mater Today 6(9):24–33
8. Khan SA, Bahadar Khan S, Ullah Khan L (2018) Fourier transform infrared spectroscopy: fundamentals and application in functional groups and nanomaterials characterization. In: Sharma S (ed) Handbook of materials characterization. Springer Nature, pp 317–344
9. Vishwanathan B, Scibioh MA (2006) Fuel cells. Hyderabad University Press.
10. Zhou C, Fang ZZ (2019) Capturing low-pressure hydrogen using V-Ti-Cr catalyzed magnesium hydride. J Power Sourc 413:139–147
11. Williams D, Carter C (2009) Transmission electron microscopy. A textbook for material science/I basics. The University of Alabama in Huntsville. USA. Springer
12. Ramaprabhu S, Rajalakshmi N (1998) Design and development of hydrogen absorption/desorption high pressure apparatus based on the pressure reduction method. Int J Hydrogen Energy 23(9):797–801
13. Liang H, Chen D (2019) Efficient hydrogen storage with the combination of metal Mg and porous nanostructured material. Int J Hydrogen Energ 44(31):16824–16832
14. Abe JO, Popoola API (2019) Hydrogen energy, economy and storage: review and recommendation. Int J Hydrogen Energy 44(29):15072–15086
15. Zheng J, Liu X, Ping Xu (2012) Development of high pressure gaseous hydrogen storage technologies. Int J Hydrogen Energ 37(1):1048–1057
16. Kalamkar R, Gangal A, Yakkundi V (2017) Development of experimental setup for measurement of stored hydrogen in solids by volumetric method. In: Pawar P, Ronge B, Balasubramaniam R, Seshabhattar S (eds) Techno-societal 2016. ICATSA 2016. Springer, Cham, pp 569–577
17. Kral L, Cermak J (2019) Improvement of hydrogen storage properties of Mg by catalytic effect of Al-containing phases in Mg-Al-Ti-Zr-C powders. Int J Hydrogen Energ 44(26):13561–13568
18. Staffell L, Scamman D (2019) The roll of hydrogen and fuel cells in the global energy system. Energ Environ Sci 12:463–491
19. Graetz J, Reilly JJ (2011) Aluminum hydride as a hydrogen and energy storage material: past, present and future. J Alloy Compd 509(2):5517–5528
20. Li M, Bai Y, Zhang C (2019) Review on the research of hydrogen storage system fast refueling in fuel cell vehicle. Int J Hydrogen Energy 44(21):10677–10693
21. Khalim Khafidz N, Yaakob Z, Timmiati SN (2019) Hydrogen sorption of magnesium oxide carbon nanofibre composite. Malaysian J Analyt Sci 23(1):60–70
22. Kale P, Gangal A, Edla R (2012) Investigation of hydrogen storage behavior of silicon nanoparticles. Int J Hydrogen Energ 37(4):3741–3747
23. Edla R, Gangal A, Manna J (2014) Kinetics and the thermal decomposition of sodium Alanate in the presence of MmNi4.5Al0.5 nanoparticles. Mater Res Express 1(1)
24. Source:https://www1.eere.energy.gov/hydrogenandfuelcells//pdfs/freedomcar_targets_explanations.pdf
25. Gao S, Wang X, He T, Yan M (2019) Effects of nano-composites (FeB, FeB/CNTs) on hydrogen storage properties of MgH_2. J Power Sourc 438:227006
26. Manoharan Y, Hosseini SE, Butler B (2019) Review: hydrogen fuel cell vehicles. current status and future prospect. Appl Sci 9(11):2296
27. Jalil Z, Rahwanto A, Ismail I (2018) The use of nano-silicon carbide and nickel as catalyst in magnesium hydrides (MgH_2) for hydrogen storage material application. Mater Res Express 5(6)
28. Beattie SD, Humphries T, Weaver L, Sean McGrady G (2008) Temporal and spatial imaging of hydrogen storage materials: watching solvent and hydrogen desorption from aluminium hydride by transmission electron microscopy. Chem Commun 37:4448–4450